

Humanoid state estimation using a moving horizon estimator

Hyoin Bae & Jun-Ho Oh

To cite this article: Hyoin Bae & Jun-Ho Oh (2017) Humanoid state estimation using a moving horizon estimator, Advanced Robotics, 31:13, 695-705, DOI: [10.1080/01691864.2017.1326317](https://doi.org/10.1080/01691864.2017.1326317)

To link to this article: <https://doi.org/10.1080/01691864.2017.1326317>



Published online: 16 May 2017.



Submit your article to this journal



Article views: 165



View related articles



CrossMark

View Crossmark data

Humanoid state estimation using a moving horizon estimator

Hyoin Bae  and Jun-Ho Oh 

Mechanical Engineering, Korea Advanced Institute of Science and Technology (KAIST), Daejeon, Republic of Korea

ABSTRACT

In this research, a new state estimator based on moving horizon estimation theory is suggested for the humanoid robot state estimation. So far, there are almost no studies on the moving horizon estimator (MHE)-based humanoid state estimator. Instead, a large number of humanoid state estimators based on the Kalman filter (KF) have been proposed. However, such estimators cannot guarantee optimality when the system model is nonlinear or when there is a non-Gaussian modeling error. In addition, with KF, it is difficult to incorporate inequality constraints. Since a humanoid is a complex system, its mathematical model is normally nonlinear, and is limited in its ability to characterize the system accurately. Therefore, KF-based humanoid state estimation has unavoidable limitations. To overcome these limitations, we propose a new approach to humanoid state estimation by using a MHE. It can accommodate not only nonlinear systems and constraints, but also it can partially cope with non-Gaussian modeling error. The proposed estimator framework facilitates the use of a simple model, even in the presence of a large modeling error. In addition, it can estimate the humanoid state more accurately than a KF-based estimator. The performance of the proposed approach was verified experimentally.

ARTICLE HISTORY

Received 10 October 2016

Revised 27 February 2017

Accepted 19 April 2017

KEYWORDS

Humanoid state estimation;
moving horizon estimation;
Kalman filter; robust state
estimation; humanoid robot;
constrained state estimation

1. Introduction

In recent years, humanoid robots of many types have been developed for various purposes. A humanoid robot is a multi-joint robot whose shape is similar to that of a human. This type of robot is regarded as the most appropriate type for collaborating with humans because its environment and the available tools are suited to human activities. Because of the advantages that humanoid robots offer, a number of research institutes have developed humanoid robots with various modes and structures. Some representative humanoid robots are HUBO, Atlas, Asimo, and HRP [1–4].

Humanoid robots are required to take on various missions in diverse environments. Accomplishment of these missions requires that robot hardware and control algorithms be developed harmoniously. One of the key requirements is a technology for estimating the robot's state (center-of-mass (COM) kinematics, attitude, contact status, etc.) rapidly and accurately. Accurate robot state estimation facilitates greater sophistication in the design of feedback controllers so that humanoid robots can respond to dynamic environments more effectively. Accordingly, many humanoid robots employ their own

state estimators. A large number of estimators are based on the Kalman filter (KF) framework [5–16].

The most basic KF-based humanoid state estimators use a linear inverted pendulum model (LIPM), which has been widely used in humanoid robot control [5–9]. The LIPM is a greatly simplified model in which humanoid movements are represented by a point mass with a constant COM height [17,18]. In [10], a force and acceleration correlation equation was employed as a KF process model, and the forward kinematics information and moment equilibrium equations were used for measurement. In [11], the base and joint velocities were estimated using a steady state KF after decoupling the full-body dynamics into base kinematics and joint kinematics. Similarly, in [12,13], the inertial measurement unit (IMU) information was added to the model input and vision information obtained through LiDAR was added as measurement data to construct the kinematics estimating KF. Another study was conducted to configure a KF for humanoid robot state estimation by applying base kinematics, foot kinematics, and gyro bias to the state vector [14]. In that study, the IMU information was used as the model input and the forward kinematics information was used as the

measurement data. Other studies have been conducted to estimate the six-degrees-of-freedom (6-DOF) dynamic deformation of the foot's flexible part, which is considered a characteristic of most humanoid robots, using a KF [15,16].

As such, a number of studies have used the KF framework for humanoid state estimation. The KF framework is widely used not only because of its optimality characteristics but also because it allows convenient implementation in a recursive discrete form [19]. However, there is a fundamental limitation to the optimality of the KF and its modifications (i.e. extended KF (EKF) [20], unscented KF [21], ensemble KF [22]). Given that elements that are not modeled are basically considered as model noise, the KF guarantees optimality only when the system model is linear, and the mean of the model noise and the measurement noise are probabilistically zero/normally distributed [23,24]. It is impossible for humanoid robots to perform accurate modeling without non-Gaussian modeling errors because they are complex multi-body/multi-joint systems. Therefore, the system model can be nonlinear. In addition, even though there are considerable constraints on humanoid robots, within the KF framework, it is difficult to incorporate equality or inequality constraints when the system model is nonlinear [25]. As a result, many of the above-mentioned studies in which KF-based state estimation is accomplished by simplifying humanoid robots into simple system models inevitably suffer from fundamental limitations.

To overcome these limitations, it is necessary to employ another type of estimator framework that is robust to nonlinear system models and modeling errors, and can accommodate constraints and model nonlinearity. This paper proposes a new approach to humanoid state estimation using a moving horizon estimator (MHE)-based method. A MHE is a type of full information (FI) estimator that can guarantee a sub-optimal solution within a finite-sized horizon window [24,26–28]. The proposed approach employs moving horizon estimation theory because it can accommodate not only nonlinear systems and various constraints, but can also partially cope with non-Gaussian modeling error (more robust to deviations from the Gaussian modeling noise). To the best of our knowledge, no studies on MHE-based humanoid state estimation have been conducted to date, despite the fact that in comparison to the KF-based approach to humanoid state estimation, the MHE-based approach can estimate a state more accurately using simple models with non-white, non-Gaussian error. In addition, an MHE-based humanoid state estimator has a simpler structure than a robust KF-based estimator [29,30], which requires the solution of complex Riccati equations. These advantages are demonstrated in this paper through simulation experiments.

The remainder of this paper is organized as follows. Section 2 briefly reviews the characteristics and features of the MHE and the KF. Section 3 describes the humanoid state estimation problem. Section 4 compares the humanoid state estimation results obtained using the proposed MHE-based estimator with that obtained using a KF-based estimator. Section 5 concludes the paper.

2. MHE and KF

In general, the purpose of state estimation is to estimate the state of a target system from a system model and given measurements. Ideally, when the system observability is valid, a globally optimal estimate can be obtained using all the measurements made up to the time when the estimate is valid (y_0, \dots, y_T , T :current time). Let x_k ($\in R_n$) be the system state vector, y_k ($\in R_m$) be the measurement vector, and subscript k denotes a discrete time step index. Then, the ideal (optimal) state estimators should solve the following problem:

$$\{x_0, \dots, x_T\}_{\text{optimal}} = \arg \max_{x_0, \dots, x_T} p(x_0, \dots, x_T | y_0, \dots, y_T) \quad (1)$$

where $p(x_0, \dots, x_T | y_0, \dots, y_T)$ is the joint probability of states x_0, \dots, x_T from the accumulated measurements. When a logarithmic transformation is applied, this maximization problem (Equation (1)) can be converted into a minimization problem, which is the computationally preferred type. Owing to this reason, by applying the logarithmic transformation and taking a conventional stochastic system model as constraints, the problem in Equation (1) can be summarized as follows.

$$\min_{x_0, \dots, x_T} \Gamma(x_0) + \sum_{k=0}^{T-1} w_k^T Q_k^{-1} w_k + \sum_{k=0}^T v_k^T R_k^{-1} v_k \quad (2)$$

$$\text{s.t.: } \Gamma(x_0) = (x_0 - \hat{x}_0)^T P_0^{-1} (x_0 - \hat{x}_0) \quad (3)$$

$$x_{k+1} = F(x_k, u_k) + w_k$$

$$y_k = h(x_k) + v_k$$

Here, $F(\cdot)$ denotes the state transition function, $h(\cdot)$ denotes the measurement function, and u_k ($\in R_p$) is the known control input vector. Furthermore, w_k ($\in R_n$, $Q_k = \epsilon [w_k w_k^T]$) is the un-modeled process error, and v_k ($\in R_m$, $R_k = \epsilon [v_k v_k^T]$) is the measurement noise. P_k ($\in R_{n \times n}$) denotes the estimate error covariance matrix.

This is usually called FI filter [26], and it can guarantee a globally optimal estimate solution. In addition, it can

accommodate not only nonlinear systems and various constraints but also non-Gaussian modeling error (robust to non-Gaussian error). If there are no constraints and the target system is linear, the estimated solution obtained using a KF is equivalent to that obtained using an FI filter. An original KF-based estimator has the following simple formulation:

Time update (prediction step)

$$\hat{x}_k^- = A_{k-1} \hat{x}_{k-1}^+ + B_{k-1} u_{k-1} \quad (4)$$

$$P_k^- = A_{k-1} P_{k-1}^+ A_{k-1}^T + Q_k \quad (5)$$

Measurement update (correction step)

$$K_k = P_k^- H_k^T (H_k P_k^- H_k^T + R_k)^{-1} \quad (6)$$

$$\hat{x}_k^+ = \hat{x}_k^- + K_k (y_k - H_k \hat{x}_k^-) \quad (7)$$

$$P_k^+ = (I - K_k H_k) P_k^- \quad (8)$$

The KF is not described in detail here. As mentioned previously, KF-based estimators have been used for humanoid state estimation in numerous studies because of the simplicity and optimality of the KF. However, for humanoid robots, highly nonlinear system models can be formulated because they are usually complex multi-body/multi-joint systems. Inevitably, non-white Gaussian modeling noise occurs. There may also be additional constraint information that is not easy to implement in the KF framework. To address these problems, a FI filter is preferred over a KF. However, with the FI filter, as more data become available (as T increases), the problem increases in size, and this can no longer be employed in real-time applications. One way to overcome this computational limitation is to reformulate the FI filter over an estimation horizon of fixed size N . This estimation approach is known as moving horizon estimation, or MHE [26–28]. Formulations of the MHE can be derived from the FI filter (Equations (2) and (3)) with a horizon size N .

$$\min_{x_{T-N+1}, \dots, x_T} \hat{\Phi}_{T-N} + \sum_{k=T-N+1}^{T-1} w_k^T Q_k^{-1} w_k + \sum_{k=T-N+1}^T v_k^T R_k^{-1} v_k \quad (9)$$

$$\text{s.t.: } x_{k+1} = F(x_k, u_k) + w_k \quad (10)$$

The basic concept of the MHE is illustrated in Figure 1. The first term in Equation (9), $\hat{\Phi}_{T-N}$, is called the arrival cost ($p(x_{k-N+1} | y_0, \dots, y_T)$) and summarizes the

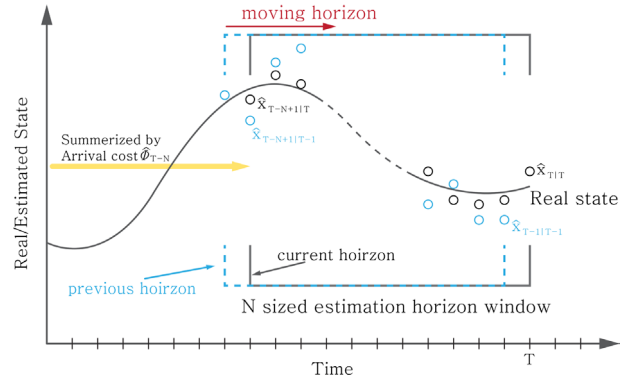


Figure 1. Basic concept of the MHE that uses an estimation horizon window of fixed size N .

past information up to the observer horizon. Several approaches have been proposed to estimate the arrival cost, such as the filtering update, smoothing update, and uniform prior approaches [24]. In this study, the uniform prior approach was selected because of its effectiveness in avoiding the multiple local optima problem that results from the use of a nonlinear system model [26,28]. A more detailed description and the effect of different choices of arrival cost upon the performance of nonlinear MHE are illustrated in [26].

3. Humanoid robot state estimation problem

This section describes a humanoid robot state estimation problem by defining the system model and its constraints. The target humanoid robot system used in this research was DRC-HUBO (Figure 2). DRC-HUBO is a humanoid robot developed by KAIST for the DARPA Robotics Challenge (DRC). It has 32 DOF, and its height and weight are 170 cm and 80 kg, respectively. It is equipped with a three-axis fiber optic gyro sensor, a three-axis accelerometer, and six-axis force torque sensors. As a result, it can detect its angular attitude and the external forces/torques of each end-effector.

It is extremely important to determine the COM movement and kinematics of humanoid robots in various dynamic situations. If COM information can be obtained accurately when creating patterns or designing controllers for biped walking algorithms, robots can operate successfully in a variety of environments. Accordingly, the objective of humanoid state estimation in this study was to estimate the COM kinematics (position/velocity) of the target humanoid robot. The linear inverted pendulum model (LIPM shown on the right-hand side of Figure 2) was adopted as the estimator model (especially for the measurement model). As shown in the figure, the LIPM is an inverted pendulum model characterized by a single point mass (m) and constant COM height (h_c). This model

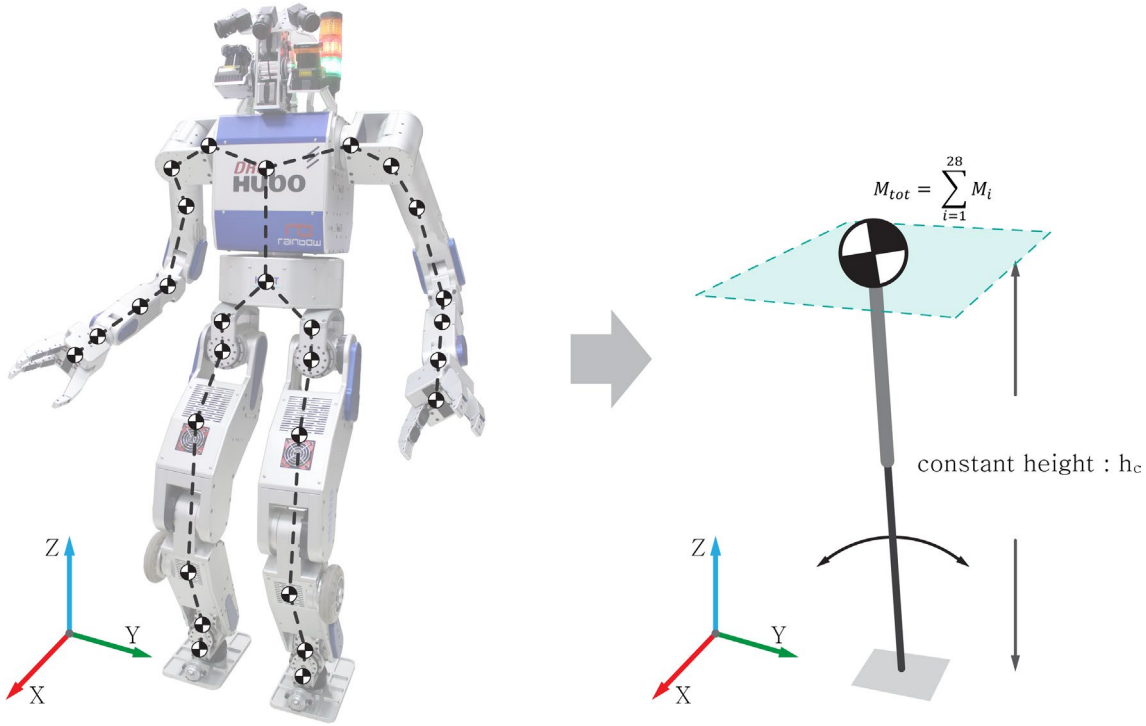


Figure 2. DRC-HUBO was used as the target humanoid robot. (Left) The model for the simulator consists of 28 rigid-body parts. (Right) A simple LIPM was used for the estimator measurement model. This was selected to focus on the comparison of the performance of the proposed MHE-based and conventional KF-based estimators. For the estimator process model, a simple nonlinear system model was adopted.

has been used in various types of algorithms for humanoid robots. Although a more complex model or full-body dynamics can improve the estimation results, they make the implementation process significantly more difficult and cause the computation time to increase exponentially. This simple model was deliberately selected for the purpose of comparing the performance of the KF-based and proposed MHE-based estimation methods. In other words, the simple LIPM model was chosen to facilitate comparison of the effects of non-zero/non-Gaussian modeling error on the KF-based and MHE-based estimators. From these purposes, the COM kinematics, body orientation, and gyro-bias defined the system state vector as follows:

$$x_k = [p_k^T v_k^T q_k^T b_k^T]^T \quad (11)$$

$$\left\{ \begin{array}{l} p_k: \text{COM position} \\ v_k: \text{COM velocity} \\ q_k: \text{body orientation} \\ b_k: \text{rate gyro bias} \end{array} \right.$$

Based on this state definition, a state transition (propagation) process could be established. The formulation of the nonlinear discrete model was based on a simple discrete

integral method and motivated by that described in [14] (Equations (12)–(15)).

$$p_{k+1} = p_k + \Delta t \cdot v_k + \frac{1}{2} \Delta t^2 \cdot (C_k^T a_k + g) \quad (12)$$

$$v_{k+1} = v_k + \Delta t \cdot (C_k^T a_k + g) \quad (13)$$

$$q_{k+1} = \exp(\Delta t \cdot \bar{w}_k) \otimes q_k \quad (14)$$

$$b_{k+1} = b_k \quad (15)$$

Here, Δt is a discrete step time, g is the gravitational acceleration, and C_k is the rotation matrix corresponding to the orientation quaternion q_k . The notation \otimes denotes quaternion multiplication, and the exponential map $\exp(\Delta w)$ relates a quaternion at times k and $k+1$, given an incremental rotation. The a_k term in Equation (13) is a measured acceleration value determined from IMU sensor data, and the \bar{w}_k term in Equation (14) is a compensated angular velocity ($\bar{w}_k = w_k - b_k w_k$: FOG measured angular velocity).

For the measurement, two values were employed: the COM position obtained from forward kinematics (y_1) and the zero-moment-point (ZMP) value calculated from the F/T sensor data (y_2). The relationship between

these two measurements and states can be formulated as follows.

$$\begin{aligned} y_k &= [y_{1,k} \ y_{2,k}]^T \\ y_{1,k} &= \text{F.K. based COM position} = p_k \end{aligned} \quad (16)$$

$$y_{2,k} = \text{Measured ZMP} = p_k - \frac{z_c}{g} C_k^T a_k \quad (17)$$

The forward-kinematics-based COM position in Equation (16) can be obtained easily through $f_{\text{forward}}(\theta_{\text{joint}}, q)$, where θ_{joint} denotes all joint angles. Equation (17) uses the conventional linear inverted pendulum model equation [17] and assumes that the acceleration of the COM is close to that of the IMU acceleration. The system model functions (Equations (12)–(15)) and measurement functions (Equations (16) and (17)) are simple but nonlinear discrete model. Accordingly, it is reasonable to expect that non-linear/non-zero/non-Gaussian modeling errors are associated with this model. For these reasons, it is an appropriate model for use in evaluating the performance of the two humanoid state estimators (the KF-based estimator and the proposed MHE-based estimator).

If there is suitable information available a priori, applying constraints can improve the estimator's performance. In the linear system, the KF and its modifications can handle equality or inequality constraints (estimate projection method, perfect measurement method, gain projection method, etc. [24]). However, in case of the nonlinear system, those estimators suffer from fundamental limitations [25]. In such systems, it is relatively easier to implement inequality (linear or nonlinear) constraints using the MHE-based estimator in contrast to the KF-based estimator [25]. In order to verify the utility of the proposed MHE-based estimator, inequality constraints are adopted in this paper.

Two straightforward inequality constraints were used in this study with the model defined above. The first constraint was a gyro bias (b_k) boundary condition and the other was a ZMP boundary condition. Rate-gyro's bias boundary condition is stated in the sensor's specification sheet. Therefore, this information can be intuitively reflected. The ZMP is constrained to be located inside the supporting polygon defined by the ground contact configuration (Figure 3). Therefore, this information can be easily applied to the biped humanoid robot. The inequality constraints can be written as follows:

$$b_{\min} < b_k < b_{\max} \quad (18)$$

$$\text{ZMP}_{\min} < p_k - \frac{z_c}{g} C_k^T a_k < \text{ZMP}_{\max} \quad (19)$$

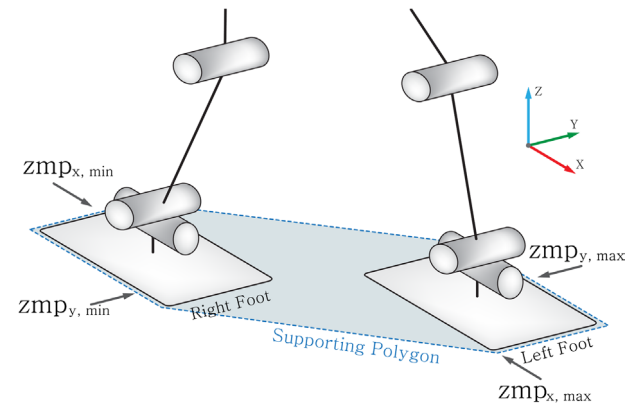


Figure 3. ZMP boundary condition. The ZMP is constrained to be located inside the supporting polygon defined by the contact foot configuration. This information can be expressed as inequality constraints.

Here, b_{\min} and b_{\max} are the minimum and maximum rate-gyro bias values indicated in the gyro manufacturer's specifications, respectively. ZMP_{\min} and ZMP_{\max} are the ZMP boundaries determined by the contact foot configuration. If more meaningful constraint information is available, more constraint equations can be applied. By combining the MHE concept (Equations (9) and (10)), the system model (Equations (12)–(17)), and the defined constraints (Equations (18) and (19)), the MHE-based humanoid state estimation framework can be constructed as follows:

- Cost functions:

$$\min_{x_{T-N+1}, \dots, x_T} \hat{\Phi}_{T-N} + \sum_{k=T-N+1}^{T-1} w_k^T Q_k^{-1} w_k + \sum_{k=T-N+1}^T v_k^T R_k^{-1} v_k \quad (20)$$

- Equality constraint:

$$x_{k+1} = F(x_k, u_k) + w_k \quad (\text{when } F: \text{Equations (12, 13, 14, and 15)}) \quad (21)$$

$$y_k = h(x_k) + v_k \quad (\text{when } h: \text{Equations (16) and (17)}) \quad (22)$$

- Inequality constraint:

$$\text{Equations (18) and (19)} \quad (23)$$

The proposed humanoid state estimator's performance was evaluated using this construction, as described in the next section.

4. Experimental results

This section describes the results of simulations conducted to evaluate the proposed MHE-based humanoid robot state estimator and a KF-based estimator, using

the same estimator model (constructed as described in the previous section). Owing to the fact that the estimator model was nonlinear, an EKF was used for the test [20]. Both estimators used the same state (Equation (11)), the same nonlinear models (Equations (12)–(17)), and the same tuning parameter values (initial values: x_0, P_0 , noise covariance matrix: Q, R). However, unlike the MHE case, inequality constraint information (Equations (18) and (19)) was not considered directly in the EKF case. Instead, estimate projection with active set method [25] was used for the inequality constrained EKF. Using this method, inequality constraints were indirectly (softly) applied in the EKF.

A simulator was used for the performance verification test instead of a real humanoid robot. The actual and estimated values should have been compared to evaluate the absolute performance of an estimator. However, it was impossible to measure the real COM accurately because of various unknown aspects of the real robot's behavior

when it is moving. Therefore, we used a simulator for the purpose of algorithm verification. The Chorenoid [31] simulator, developed by AIST, was used in this study. To simulate the target humanoid robot (DRC-HUBO, Figure 2), the robot was divided into 28 rigid-body parts.

The simulator was used to simulate the walking motion of the humanoid robot. This specific motion was chosen because bipedal locomotion is a fundamental and challenging problem for humanoid robots. The simulation is illustrated in Figure 4. The robot took 10 steps, each of them 10 cm in length. The walking algorithm for this test was based on [32]. Force/torque data, rate gyro data, acceleration data, and joint angles were recorded during the simulation. Using these data, the two estimators were used to estimate the COM kinematics. Overall estimation performance evaluation system's schematic diagram is shown in Figure 5. As shown in the figure, mass and link information were intentionally distorted in order to generate modeling error (modeling disturbance) in the

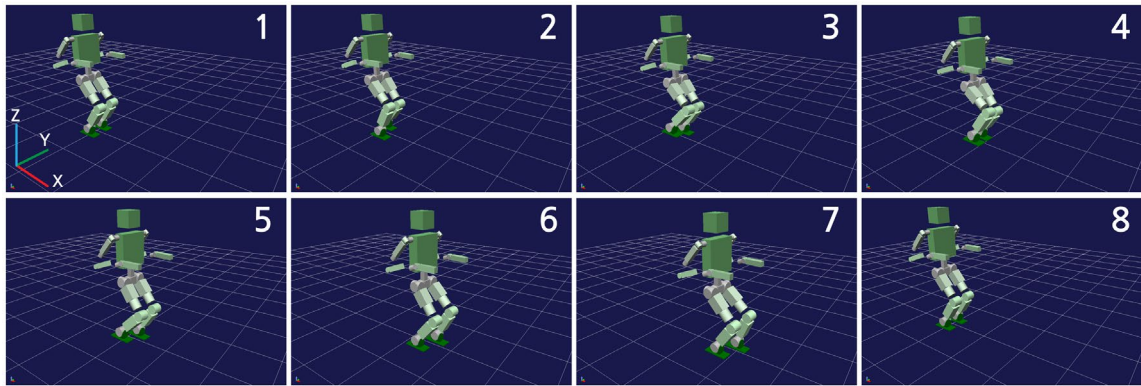


Figure 4. Humanoid robot walking in the Chorenoid simulator. The robot took 10 steps, each 10 cm in length, and COM estimation was performed using the data obtained.

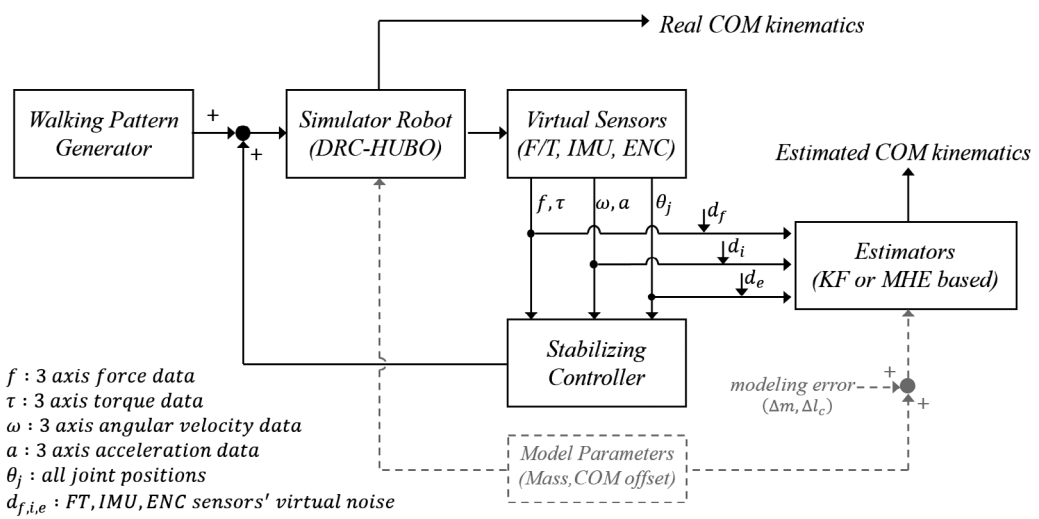


Figure 5. Overall estimation performance evaluation test's schematic diagram. Mass, link length, and COM-offset information were intentionally distorted to generate the un-modeled modeling error.

estimator. Control and sampling frequency of this simulator was 200 Hz ($\Delta t = 0.005$ ms).

The estimation results for the KF-based and MHE-based estimators are shown in Figures 6–8. Figure 6 shows the estimation results for the humanoid robot COM along

the x -axis. The left-hand side of Figure 6 shows the entire walking sequence result, and the right-hand side shows a magnified view of a particular time interval. Figure 7 shows the estimation results for the humanoid robot COM along the y -axis. Similar to the x -axis graph (Figure 6),

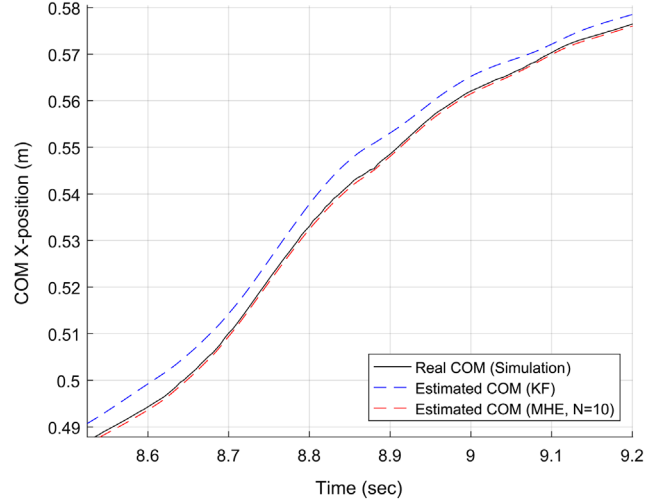
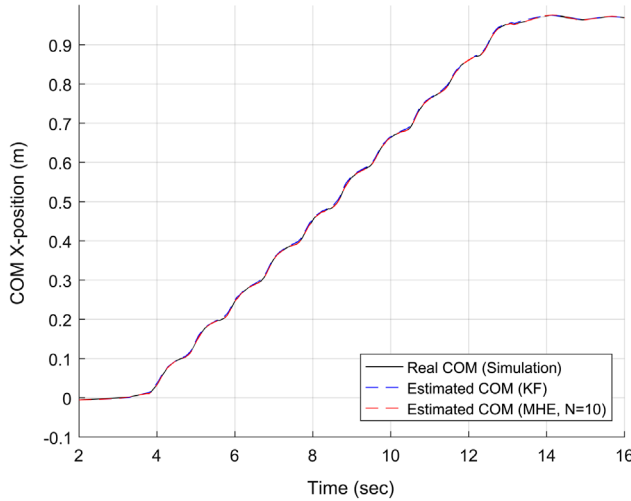


Figure 6. Comparison between true COM value along the x -axis and values estimated using the KF-based estimator and the proposed MHE-based estimator.

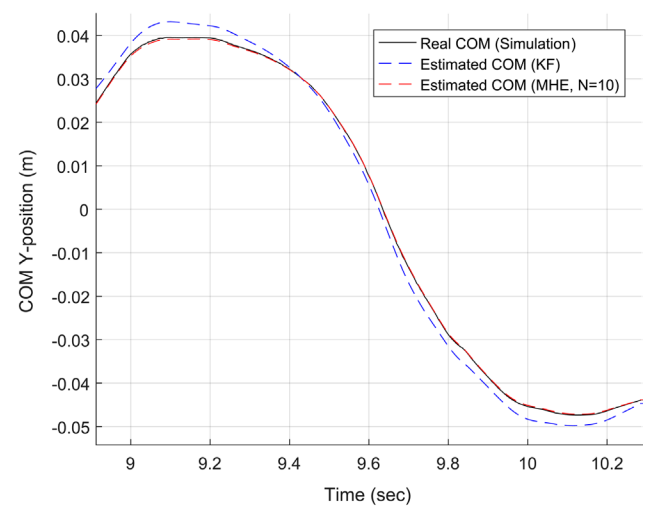
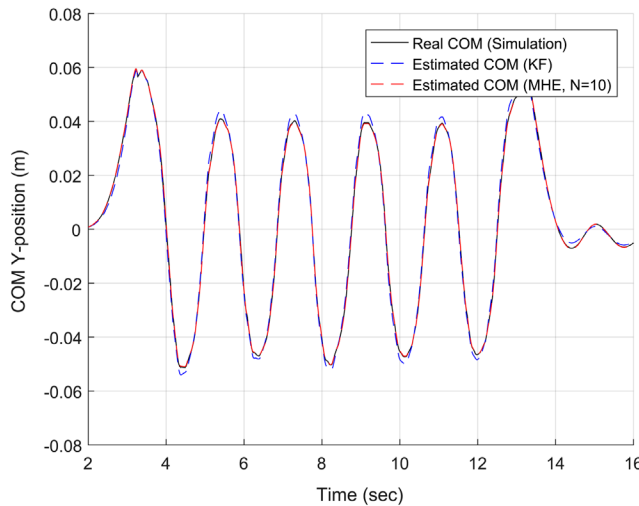


Figure 7. Comparison between true COM value along the y -axis and values estimated using the KF-based estimator and the proposed MHE-based estimator.

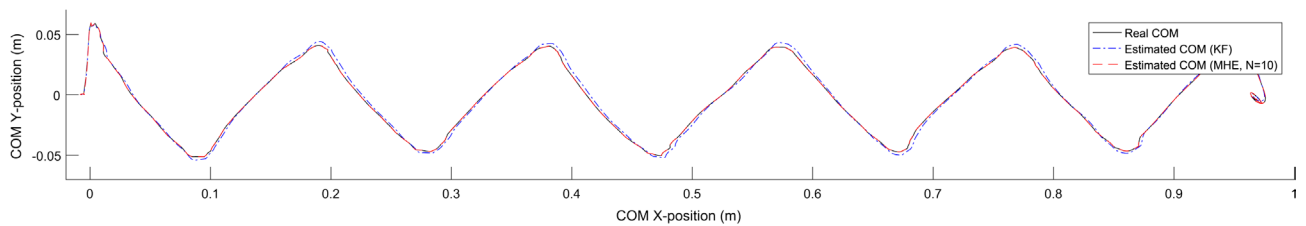


Figure 8. Comparison between true COM value and values estimated using the KF-based estimator and the proposed MHE-based estimator.

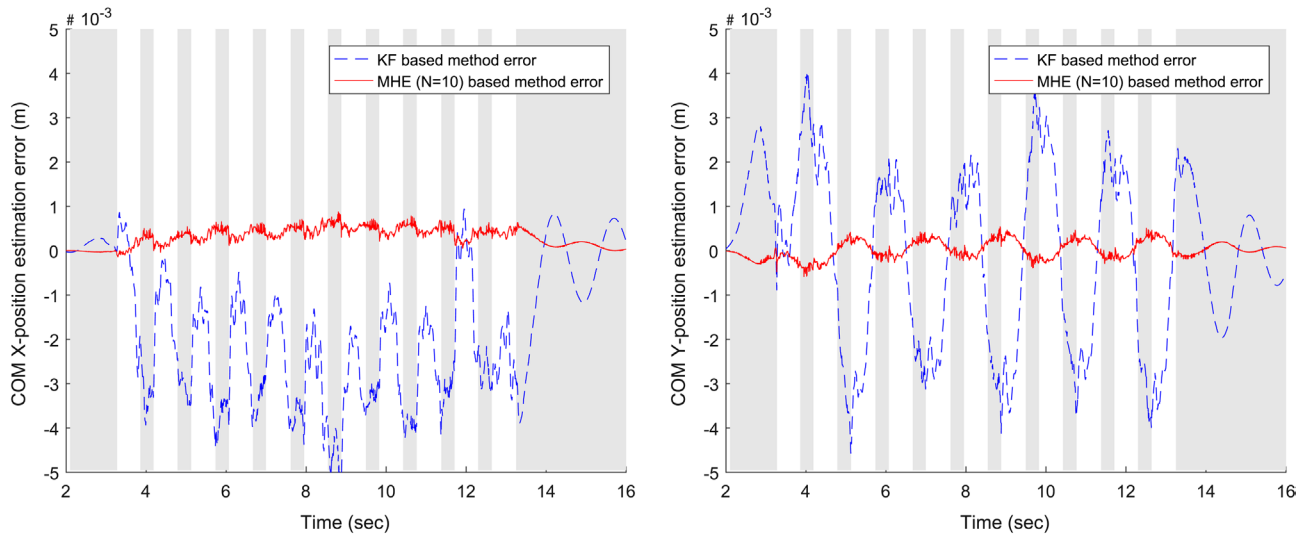


Figure 9. (Left) Estimation error along the x-axis for the two estimators (Right) Estimation error along the y-axis for the two estimators. In both directions, the proposed MHE-based estimator reproduced the COM kinematics more accurately than the KF-based humanoid state estimator. The gray region represents the double-support phase (DSP), in which both feet are on the ground while walking.

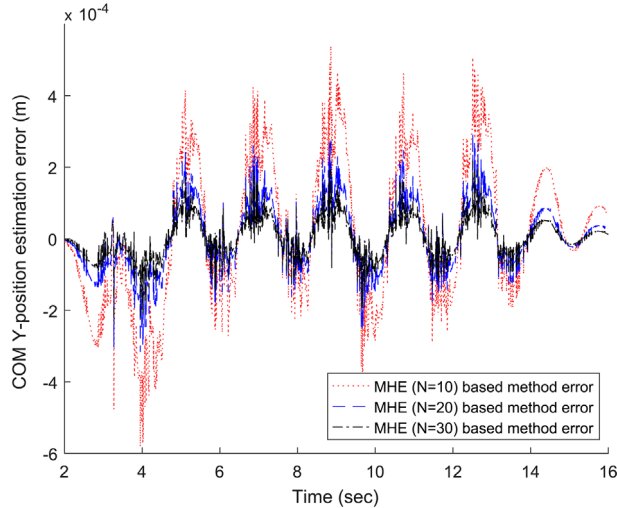


Figure 10. Influence of the moving horizon estimation window size N . Increasing horizon size results in better estimation performance.

the left-hand side of Figure 7 shows the entire walking sequence result, and the right-hand side shows a magnified view of a particular time interval. In each figure, the black solid line represents the real COM x -axis or y -axis position obtained from the simulator. The blue and red dashed lines represent the KF-based estimator output and the MHE-based estimator output, respectively. In the case of the MHE-based estimator, we set the estimation horizon window size to 10 steps ($N = 10$). MHE estimation horizon size was determined based on our intuition. This size was chosen to provide a trade-off between estimation accuracy and computational effort. Effect of the size of the horizon will be discussed later. For the MHE

Table 1. Comparison of performance of the KF-and MHE-based estimators.

	KF (EKF)	MHE ($N = 10$)	MHE ($N = 20$)	MHE ($N = 30$)
RMS error	1.6118	0.1622	0.0744	0.0473
Peak error	3.9202	0.5395	0.2949	0.2174
Relative computation cost	<<1	0.88	0.94	1

Note: Direction: y-axis, units: mm.

optimization problem, Matlab's Quadprog optimizer was used. The X-Y horizontal plane view of these results is illustrated in Figure 8.

The simulation test results shown in Figures 6–8 indicate that the proposed MHE-based humanoid state estimator estimated the true COM kinematics more accurately than the KF-based estimator. This improved performance can be observed from Table 1 and Figure 9. Using the proposed MHE-based estimator, the root-mean-square (RMS) error and peak-error decreased by approximately 90 and 86%, respectively, as compared to the EKF estimator. This can be attributed to the fact that the MHE can accommodate the nonlinearity of the system and the state inequality constraints. In addition, the MHE-based estimator can handle the non-Gaussian modeling error generated by the selected simple nonlinear system model effectively and robustly. On the other hand, the KF-based estimator was not robust to factors such as the nonlinear system, non-Gaussian modeling error, and constraints, as expected. Figure 9 shows the errors between the actual COM position and the estimated values in the two axis directions.

As shown previously in Figures 6–8, the MHE-based method produces more precise results (close to zero-error

value) compared to the KF-based method. The gray colored region in Figure 9 represents the double supporting phase (DSP), in which both feet are on the ground while walking. The KF-based method suffers from large modeling errors in the DSP sections, where a large impact force comes from the ground because of foot contact.

Figure 10 illustrates the influence of the moving horizon window size N on the MHE-based estimation results

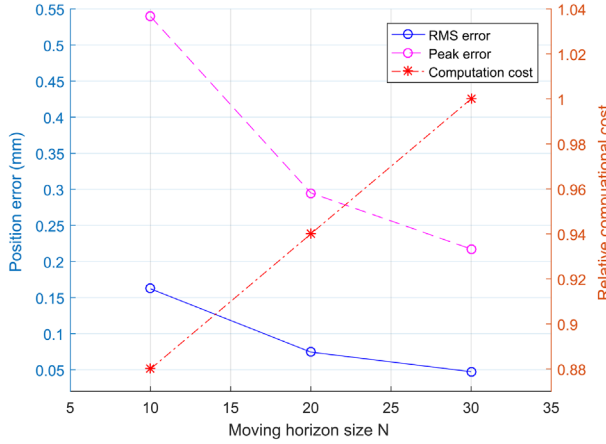


Figure 11. Influence of the moving horizon estimation window size N on RMS/peak errors and the relative computational time.

for the y -axis COM position estimation error. Increasing the horizon size yields better estimation performance (Table 1). However, a larger horizon size may increase the computational cost. The RMS errors, maximum errors, and relative computational costs associated with the use of the KF-based and MHE-based estimators for three values of N are shown in Table 1 and Figure 11.

The results show that the proposed MHE-based humanoid state estimator exhibits better state estimation performance in comparison with the KF-based estimator for the simple nonlinear model used here.

In order to verify the feasibility of the proposed MHE-based estimator, the algorithm was implemented on a real robot platform. COM estimation results obtained using the proposed MHE-based estimator with real humanoid robot are shown in Figure 12. In this experiment, a real DRC-HUBO was used as the humanoid robot platform. It took eight forward steps, each of them 15 cm in length, thus covering a distance of 1.2 m. However, we could not acquire the actual COM position (ground-truth value) accurately in the real environment because of various unknown aspects of the real robot's behavior in motion. Therefore, the actual COM position is not shown in the result figure. However, from the result, it can be observed that the proposed MHE-based state estimator can produce

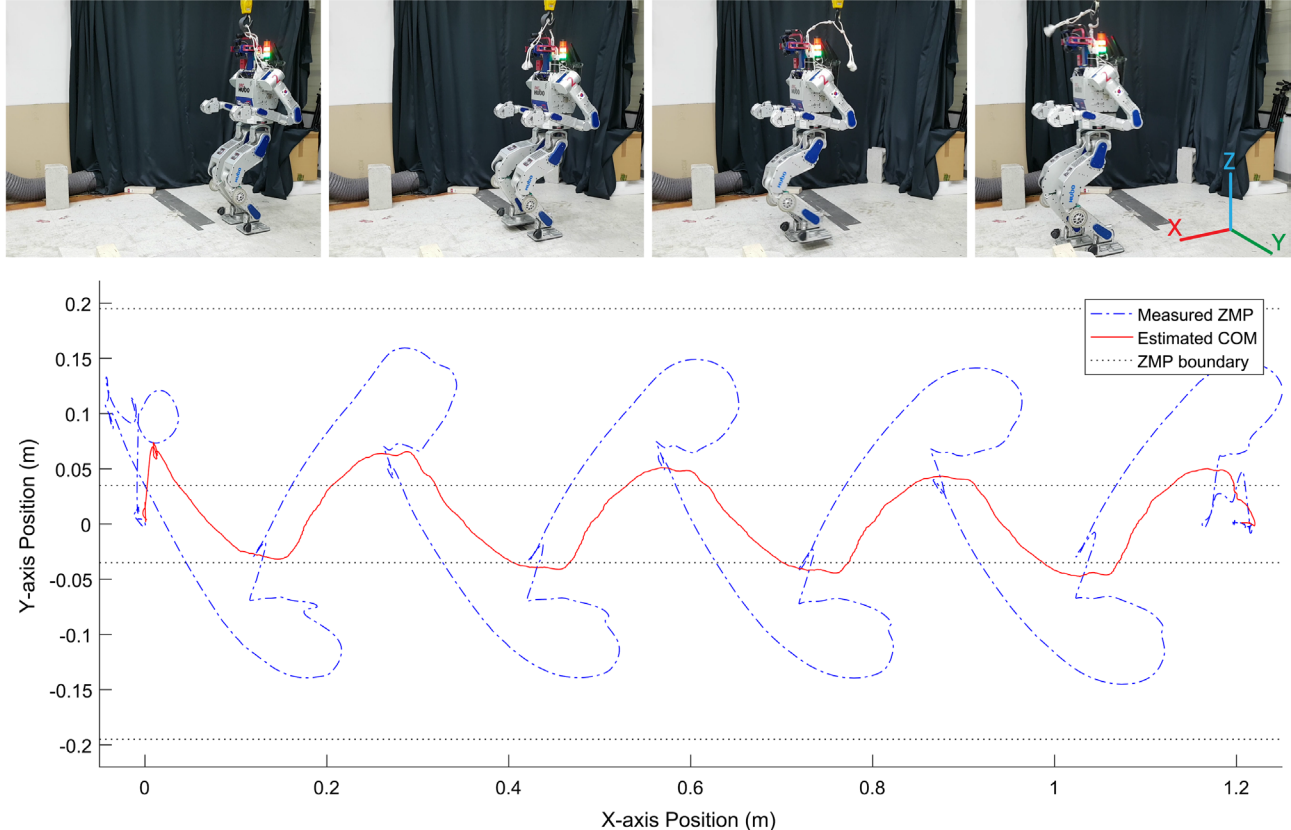


Figure 12. COM position (x and y axes) estimation result using the proposed MHE-based estimator with the real humanoid robot DRC-HUBO. The robot took eight steps, each 15 cm in length, and COM estimation was performed in real-time.

smooth and continuous estimated values, and did so in real-time. Compare with the simulation result figure (Figure 8), it shows a similar COM estimate pattern.

5. Conclusion

This paper proposes the use of a MHE in humanoid state estimation to overcome the inherent limitations of KF-based estimators. Conventional KF-based estimators can guarantee optimal estimation results only if the system is linear and the modeling errors follow a Gaussian distribution. However, it is impossible for humanoid robots to perform accurate modeling without taking into consideration non-Gaussian modeling errors because they are complex/nonlinear multi-body/multi-joint systems. In addition, even though there are considerable constraints on humanoid robots, it is difficult to incorporate equality or inequality constraints within the KF framework. This is especially true when the estimator model is nonlinear. As a result, the various KF-based humanoid state estimators that have been proposed in previous studies suffer from fundamental limitations. In contrast to KF-based estimators, the proposed MHE-based estimator can accommodate nonlinear systems and various constraints, while being more robust to non-Gaussian modeling errors. Therefore, the proposed MHE-based humanoid state estimator can yield more accurate and robust estimation results when compared with KF-based humanoid state estimators. The superiority of the MHE-based method was verified through simulation using a simple nonlinear model. In particular, the proposed estimator performed better in dynamic situations with substantial modeling noise.

The theoretical derivation and experimental results show that the proposed MHE is a viable alternative to KF-based estimators for humanoid state estimation. In this study, a relatively simple nonlinear model was used intentionally to evaluate the performance of the proposed estimator. However, the applicability of this model is extremely limited. Therefore, in the future, we plan to design a more accurate and systematic estimator structure and model based on the proposed MHE-based approach to model various humanoid motions.

Disclosure statement

No potential conflict of interest was reported by the authors.

Funding

This work was supported by ‘Development of core technologies and a standard platform for humanoid robot [10060103]’, project from the Ministry of Trade, Industry and Energy (MOTIE) of the Republic of Korea.

Notes on contributors

Hyoin Bae received his BS degree in Mechanical Engineering from Korea Advanced Institute of Science and Technology (KAIST), Daejeon, South Korea, and MS in Mechanical Engineering from KAIST, in 2012 and 2014, respectively. Since 2014, he has been pursuing the PhD degree in Mechanical Engineering at the KAIST and working on the project of development for humanoid robots: HUBO2 and DRC-HUBO. His research interests include state estimation for multi degree of freedom system, disturbance estimation, humanoid robot design, and sensor fusion algorithm.

Jun-Ho Oh received his BS and MS degrees in Mechanical Engineering from Yonsei University, Seoul, South Korea, and PhD degree in Mechanical Engineering from University of California, Berkeley, in 1977, 1979, and 1985, respectively. He was a researcher with the Korea Atomic Energy Research Institute from 1979 to 1981. Since 1985, he has been with the Department of Mechanical Engineering, KAIST, where he is currently a significant professor and a director of Humanoid Robot Research Center. Moreover, he has been a vice president of KAIST since 2013. He was a Visiting Research Scientist in the University of Texas Austin from 1996 to 1997. His research interests include humanoid robots, adaptive control, intelligent control, nonlinear control, biomechanics, sensors, actuators, and application of micro-processor. Oh is a member of the IEEE, KSME, KSPE, and ICASE.

ORCID

Hyoin Bae  <http://orcid.org/0000-0003-4050-2147>

Jun-Ho Oh  <http://orcid.org/0000-0002-2609-6712>

References

- [1] Park I-W, Kim J-Y, Oh J-H, et al. Mechanical design of humanoid robot platform KHR-3 (KAIST humanoid robot 3: HUBO). Proceedings of the 5th IEEE-RAS International Conference on Humanoid Robots; 2005 Dec 5–7; Tukuba, Japan. IEEE; 2005. p. 321–326.
- [2] Johnson M, Shrewsbury B, Bertrand S, et al. Team IHMC’s lessons learned from the DARPA robotics challenge trials. J Field Robot. 2015;32(2):192–208.
- [3] Hirose M, Ogawa K. Honda humanoid robots development. Philos Trans Roy Soc London A. 1985;2007(365):11–19.
- [4] Kaneko K, Harada K, Kanehiro F, et al. Humanoid robot HRP-3. Proceedings of the IEEE/RSJ International Conference on Intelligent Robots and Systems; 2008 Sep 22–26; Nice, France. IEEE; 2008. p. 2471–2478.
- [5] Park S, Han Y, Hahn H. Kalman filter based zmp estimation scheme for balance control of a biped robot. Proceedings of the 4th International Conference on Ubiquitous Robots and Ambient Intelligence; 2007 Nov 14–16; Pohang, Korea. IEEE; 2007.
- [6] Kwon SJ, Oh Y. Estimation of the center of mass of humanoid robot. Proceedings of the International Conference on Control, Automation and Systems; 2007 Oct 17–20; Seoul, Korea. IEEE; 2007. p. 2705–2709.

- [7] Xinjilefu X, Atkeson CG. State estimation of a walking humanoid robot. Proceedings of the IEEE/RSJ International Conference on Intelligent Robots and Systems; 2012 Oct 7–12; Vilamoura-Algarve, Portugal. IEEE; 2012. p. 3693–3699.
- [8] Xinjilefu X, Feng S, Atkeson CG. Center of mass estimator for humanoids and its application in modelling error compensation, fall detection and prevention. Proceedings of the 15th IEEE-RAS 15th International Conference on Humanoid Robots; 2015 Nov 3–5; Seoul, Korea. IEEE; 2015. p. 67–73.
- [9] Wittmann R, Hildebrandt AC, Wahrmann D, et al. State estimation for biped robots using multibody dynamics. Proceedings of the IEEE/RSJ International Conference on Intelligent Robots and Systems; 2015 Sep 28–Oct 2; Hamburg, Germany. IEEE; 2015. p. 2166–2172.
- [10] Masuya K, Sugihara T. COM motion estimation of a Humanoid robot based on a fusion of dynamics and kinematics information. Proceedings of the IEEE/RSJ International Conference on Intelligent Robots and Systems; 2015 Sep 28–Oct 2; Hamburg, Germany. IEEE; 2015. p. 3975–3980.
- [11] Xinjilefu X, Feng S, Huang W, et al. Decoupled state estimation for humanoids using full-body dynamics. Proceedings of the IEEE International Conference on Robotics and Automation; 2014 May 31-Jun 07; Hong Kong, China. IEEE; 2014. p. 195–201.
- [12] Fallon MF, Antone M, Roy N, et al. Drift-free humanoid state estimation fusing kinematic, inertial and lidar sensing. Proceedings of the IEEE-RAS International Conference on Humanoid Robots; 2014 Nov 18–20; Madrid, Spain. IEEE; 2014. p. 112–119.
- [13] Kuindersma S, Deits R, Fallon M, et al. Optimization-based locomotion planning, estimation, and control design for the atlas humanoid robot. Auton Robots. 2015;40(3):429–455.
- [14] Rotella N, Bloesch M, Righetti L, et al. State estimation for a humanoid robot. Proceedings of the IEEE/RSJ International Conference on Intelligent Robots and Systems; 2014 Sep 14–18; Chicago (IL): IEEE; 2014. p. 952–958.
- [15] Benallegue M, Lamiraux F. Humanoid flexibility deformation can be efficiently estimated using only inertial measurement units and contact information. Proceedings of the IEEE-RAS International Conference on Humanoid Robots; 2014 Nov 18–20; Madrid, Spain. IEEE; 2014. p. 246–251.
- [16] Mifsud A, Benallegue M, Lamiraux F. Estimation of contact forces and floating base kinematics of a humanoid robot using only Inertial Measurement Units. Proceedings of the IEEE/RSJ International Conference on Intelligent Robots and Systems; 2015 Sep 28–Oct 2; Hamburg, Germany. IEEE; 2015. p. 3374–3379.
- [17] Kajita S, Kanehiro F, Kaneko K, et al. The 3D linear inverted pendulum mode: a simple modeling for a biped walking pattern generation. Proceedings of the IEEE/RSJ International Conference on Intelligent Robots and Systems; 2001 Oct 29–Nov 3; Hawaii, USA. IEEE; 2001. p. 239–246.
- [18] Kajita S, Kanehiro F, Kaneko S, et al. A realtime pattern generator for biped walking. Proceedings of the IEEE International Conference on Robotics and Automation; 2002 May 11–15; Washington (DC): IEEE; 2002. p. 31–37.
- [19] Welch G, Bishop G. An Introduction to the Kalman Filter; 1995.
- [20] Terejanu GA. Extended Kalman filter tutorial. University at Buffalo; 2008.
- [21] Julier SJ, Uhlmann JK. New extension of the Kalman filter to nonlinear systems. Orlando (FL): SPIE; 1997.
- [22] Evensen G. The ensemble Kalman Filter: theoretical formulation and practical implementation. Ocean Dyn. 2003;53(4):343–367.
- [23] Andrews AP. Kalman filtering: theory and practice using MATLAB; 2001.
- [24] Simon Dan. Optimal state estimation. Wiley; 2006.
- [25] Simon Dan. Kalman filtering with state constraints: a survey of linear and nonlinear algorithms. IET Control Theory Appl. 2010;4(8):1303–1318.
- [26] Haseltine EL, Rawlings JB. A critical evaluation of extended Kalman filtering and moving horizon estimation. Ind Eng Chem Res 2005;44(8):2451–2460.
- [27] Rao CV, Rawlings JB, Mayne DQ. Constrained state estimation for nonlinear discrete-time systems: stability and moving horizon approximations. IEEE Trans Autom Control. 2003;48(2):246–258.
- [28] Rao CV, Rawlings JB, Lee JH. Constrained linear state estimation – a moving horizon approach. Automatica. 2001;37(10):1619–1628.
- [29] Gu D-W, Poon FW. A robust state observer scheme. IEEE Trans Autom Control. 2001;46(12):1958–1963.
- [30] Yang F, Wang Z, Hung YS. Robust Kalman filtering for discrete time-varying uncertain systems with multiplicative noises. IEEE Trans Autom Control. 2002;47(7):1179–1183.
- [31] Chorenoid.org [Internet]. Japan: AIST; [cited 2016 Aug 15]. Available from: <http://chorenoid.org/en/>
- [32] Heo J-W, Oh J-H. Biped walking pattern generation using an analytic method for a unit step with a stationary time interval between steps. IEEE Trans Industr Electron. 2015;62(2):1091–1100.